Proc. Natl. Acad. Sci. USA
Vol. 84, pp. 5730–5734, August 1987
Biophysics

Structure of the reaction center from *Rhodobacter sphaeroides* R-26: The cofactors*

(bacterial photosynthesis/membrane protein structure/x-ray diffraction/membrane protein)

J. P. ALLEN†, G. FEHER†‡, T. O. YEATES§, H. KOMIYA§, AND D. C. REES§

†University of California, San Diego, La Jolla, CA 92093; and §University of California, Los Angeles, CA 90024

Contributed by G. Feher, May 4, 1987

ABSTRACT **The three-dimensional structure of the cofactors of the reaction center of *Rhodobacter sphaeroides* R-26 has been determined by x-ray diffraction and refined at a resolution of 2.8 Å with an *R* value of 26%. The main features of the structure are similar to the ones determined for *Rhodopseudomonas viridis* [Michel, H., Epp, O. & Deisenhofer, J. (1986) *EMBO J.* 5, 2445–2451]. The cofactors are arranged along two branches, which are approximately related to each other by a 2-fold symmetry axis. The structure is well suited to produce light-induced charge separation across the membrane. Most of the structural features predicted from physical and biochemical measurements are confirmed by the x-ray structure.**

The reaction center (RC) is an integral membrane protein–pigment complex that mediates the primary processes of photosynthesis—i.e., the light-induced electron transfers from a donor to a series of acceptor species. The three-dimensional structure of the RC from the photosynthetic bacterium *Rhodopseudomonas viridis* has recently been determined by x-ray diffraction at a resolution of 2.9 Å (1–3). In this paper, we report the structure analysis of the RC from another purple bacterium, the carotenoidless mutant R-26 of *Rhodobacter sphaeroides* (previously called *Rhodopseudomonas sphaeroides*). The motivation for undertaking the structure determination of the RC of a second bacterial species was 2-fold. (*i*) The RC from *Rb. sphaeroides* has been investigated for the past two decades and, consequently, is the best characterized RC (for reviews see refs. 4 and 5); in addition, the methodologies for manipulating its structure (e.g., exchanging cofactors, dissociating and reassociating the subunits) have been worked out in detail (4–10). (*ii*) The availability of structures from two organisms may help in elucidating structure–function relationships by correlating differences in structure with differences in function.

The RC from *Rb. sphaeroides* is composed of three protein subunits—L, M, and H—and the following cofactors: four bacteriochlorophylls (Bchls), two bacteriopheophytins (Bphes), two ubiquinones, and one nonheme iron. The RC from *R. viridis* has an additional subunit, a cytochrome with four *c*-type hemes; its Bchls and Bphes are of the "b" type instead of the "a" type found in *Rb. sphaeroides*, and its primary quinone is a menaquinone. Notwithstanding these differences, the two structures were found to be very similar. This made it possible to use the method of molecular replacement (11) to solve the phase problem in the x-ray analysis (12–14). The crystals of *Rb. sphaeroides* diffract at least to a resolution of 2.6 Å and retain the ability to perform the primary photochemistry (15). We have solved the structure of the protein and the cofactors to a resolution of 2.8 Å with an *R* factor of 26%. In this paper, we report the structure of the cofactors. The structure of the protein, the relation of the RC protein to the membrane, and the interaction of the cofactors with the protein will be reported in subsequent publications (52, 53). Preliminary accounts of this work have been presented (12, 14–18).

EXPERIMENTAL PROCEDURES

Crystallization and Data Collection. The RC from *Rb. sphaeroides* has been crystallized in various space groups (15) including the form (space group $P2_12_12_1$) used in this work (18). The crystals were grown by vapor diffusion in the presence of the detergent lauryl dimethyl amine oxide (LDAO) as described (14, 17). The crystals often exhibited additional weak reflections, which could be indexed on a C-centered lattice, with a doubling of the *a* and *b* axes. The presence of these additional reflections indicates a short-range orientational disorder in the crystal packing (19, 20). This disorder was suppressed by replacing through dialysis the detergent LDAO in the crystallization buffer with octyl β-glucoside after the crystal was fully grown. All crystals described in this work were treated this way.

Initially, we analyzed a data set at 3.3 Å resolution obtained from two crystals with a multiwire area detector (21) mounted on a GX-21 rotating anode x-ray generator. The DIFCOR program of the ROCKS crystallographic computing package (22) was used to merge the data. The *R* factor (defined as $R = \Sigma|I_i - I_j|/\Sigma|I_i + I_j|$, where the measured intensities *I* are summed over all symmetry-related reflections *i* and *j*) for merging this data set was 6.8%. More recently, we have collected data on a rotation camera to a resolution of 2.8 Å at the Brookhaven National Laboratory Synchrotron facility. Films were scanned with the SCAN12 package (23) and the intensities were merged using DIFCOR resulting in an R factor of 8.9%. A total of 23,349 unique reflections (62% of maximum) with intensities exceeding twice the standard deviation were measured.

Data Refinement. An initial analysis of the structure of the RC from *Rb. sphaeroides* had been performed using the molecular replacement method (12, 14, 17). However, the replacement of the detergent, as discussed above, changed the unit cell dimensions from 142.4, 75.5, and 141.8 Å to 138.0, 77.5, and 141.8 Å for *a*, *b*, and *c*, respectively. Consequently, the original rigid body and unit cell parameters of the RC model needed to be refined. The refinement resulted in a rotation of the model by 1.9° and a translation of the center of mass by 1.4 Å. The *R* factor between observed and calculated structure factors was 43% for the data between 8 Å and 3.5 Å resolution.

The publication costs of this article were defrayed in part by page charge payment. This article must therefore be hereby marked "*advertisement*" in accordance with 18 U.S.C. §1734 solely to indicate this fact.

Abbreviations: RC, reaction center; $Bchl_2$, bacteriochlorophyll dimer; $(Bchl_2)_A$ and $(Bchl_2)_B$, tetrapyrrole rings closer to the A and B branches, respectively; Bphe, bacteriopheophytin; $Bphe_A$ and $Bphe_B$, Bphe branches A and B, respectively; Q_A and Q_B, primary and secondary quinones, respectively.

*This is paper no. 1 in a series. Papers nos. 2 and 3 are references 52 and 53, respectively.

‡To whom reprint requests should be addressed.

Atomic refinement of the RC model was performed with the restrained least-squares program PROLSQ of Hendrickson and Konnert as discussed in ref. 24. Structure factor derivatives were determined from the differences in the observed and calculated electron density maps with the DERIV program (25). Individual temperature factors (B) were refined in subsequent refinement cycles. We used as an initial structure for the RC from *Rb. sphaeroides* the structure of the RC from *R. viridis* with the cytochrome removed and the nonconserved residues replaced by alanine (14). Refinement cycles were alternated with model building (i.e., the replacement of alanines with the proper residues in the nonconserved positions) using an interactive graphics terminal (Evans and Sutherland PS 300) and the program FRODO (26). At the present stage of refinement, the R factor between observed and calculated structure factors is 26% for the data between 6 Å and 2.8 Å resolution. The root-mean-square (rms) deviations from standard bond distances and angles are 0.02 Å and 5°, respectively. All residues were built into the electron density, except for six residues at the carboxyl terminus of the L subunit and residues 48–53 of the H subunit.

Luzzati plots (27) of the R factor as a function of resolution indicate an average rms error in the coordinates of 0.4 Å. Analysis of the average temperature coefficient B for each residue suggests that the transmembrane region of the RC structure is better defined than the regions exposed to the solvent. The higher B values in the solvent-exposed regions reflect either increased flexibility or an uncertainty in the atomic positions. Refinement at higher resolution is expected to improve the detail with which the RC structure will be determined.

RESULTS AND DISCUSSION

General Organization of the Cofactors. The cofactors of the RC from *Rb. sphaeroides* are arranged along two branches called A and B,¶ which are approximately related to each other by a 2-fold symmetry axis, as has been previously found in *R. viridis* (1) (see Figs. 1 and 2). The arrangement of pigments along branch A is in accord with the electron pathway as predicted from spectroscopic measurements (for reviews, see refs. 28 and 29)—i.e., the primary donor $Bchl_2$ is followed by Bchl, Bphe, and a quinone. The distances and angles between the cofactors are presented for both species in Table 1. The positions of the centers of the tetrapyrrole rings are well conserved; there are, however, some differences in the relative orientation of the rings and the placement of the side chains. For both species, the acetyl groups on ring I of the six tetrapyrroles lie approximately in the plane of the ring. The positions of the primary quinones differ, although this may be partially due to the difference between ubiquinone (in *Rb. sphaeroides*) and menaquinone (in *R. viridis*). Comparison cannot be made between the two Q_Bs since the secondary quinone has apparently been lost in the RC from *R. viridis*.

The line joining the center of the dimer $Bchl_2$ and the Fe atom represents only an approximate 2-fold symmetry axis. To obtain the best rotation axis that relates equivalent cofactors in the two branches, a transformation matrix was determined by a least-squares method, which optimized the superposition of the cofactors of the A branch onto the cofactors of the B branch (30). The rotation axis obtained from this transformation matrix is specified by the polar angles $\phi = 81°$, $\psi = 52°$, and $\kappa = 183°$ (see ref. 14 for definition of angles). For this transformation, the rms deviation between equivalent atoms was 0.7 Å for $Bchl_2$, 1.3 Å for Bchl, 1.4 Å for Bphe, and 2.2 Å for the quinones. Thus, in terms of function, the cofactors that are involved in the more primary processes obey the 2-fold symmetry better than those involved in the later stages.

Table 1. Parameters relating neighboring cofactors of RC from *Rb. sphaeroides** and *R. viridis*†

Cofactors	Distance between ring centers, Å‡		Angle between ring normals§	
	Rb. sph.	*R. vir.*	*Rb. sph.*	*R. vir.*
$(Bchl_2)_A$; $(Bchl_2)_B$	7.0	7.0	10°	15°
$(Bchl_2)_A$; $Bchl_A$	11.0	10.5	70°	65°
$(Bchl_2)_B$; $Bchl_B$	10.5	11.0	70°	70°
$Bchl_A$; $Bphe_A$	10.5	10.0	60°	70°
$Bchl_B$; $Bphe_B$	11.0	11.0	60°	70°
$Bphe_A$; Q_A	13.0	14.0	35°	35°
$Bphe_B$; Q_B	15.0	NA	35°	NA
Q_A; Q_B	18.5	NA	20°	NA
Fe; Q_A	11.0¶	9.0¶	NA	NA
Fe; Q_B	8.0¶	NA	NA	NA

Rb. sph., Rb. sphaeroides; R. vir, R. viridis; NA, not applicable.
*This work.
†From ref. 14.
‡Ring centers are the centeroids of the cofactor ring system. Estimated error of the coordinates is ± 0.4 Å.
§Normal to the plane of the cofactor ring system (obtained by a least squares fit); estimated error for tetrapyrrole rings, ±6° and for quinones, ±15°.
¶Distance from Fe to center between the two carbonyl oxygens.

The phytyl chains of the tetrapyrrole rings and the isoprenoid chain of Q_A are also approximately conserved in the two species. There are, however, two obvious differences. First, the phytyl chain of $Bchl_A$ of *Rb. sphaeroides* is directed away from the other cofactors, but for *R. viridis*, this chain loops toward Q_A (see Fig. 1). Second, the phytyl chain of $Bchl_B$ of *Rb. sphaeroides* is approximately in a symmetry-related position to that of $Bchl_A$. In *R. viridis*, this chain extends down toward the putative position of Q_B. The placement of this chain is surprising since in *Rb. sphaeroides* such a placement would interfere with the isoprenoid chain of Q_B. This placement implies either a different location of Q_B in *R. viridis* or a structural change that resulted from the removal of Q_B in *R. viridis*.

We next consider the overlaps of the van der Waals surfaces between phytyl and isoprenoid chains and the pigments. These may play a role in the electron transfer processes. A striking demonstration of the ability of hydrocarbon chains to conduct electrons has recently been reported (31). The phytyl chain of $(Bchl_2)_A$ contacts both the tetrapyrrole rings of $Bchl_A$ and $Bphe_A$, whereas $(Bchl_2)_B$ contacts only $Bphe_B$. The phytyl chain of $Bchl_A$ has no contacts with other cofactors, whereas $Bchl_B$ contacts $Bphe_B$. The isoprenoid chain of Q_A, contacts the phytyl chain of $Bchl_A$, whereas the isoprenoid chain of Q_B is in contact with the tetrapyrrole ring of $Bphe_B$. Except for the differences noted previously, these features are conserved in *R. viridis*.

The $Bchl_2$ Dimer. The identification of $Bchl_2$ as the primary donor was obtained from EPR and electron nuclear double resonance (ENDOR) experiments. The EPR line width of the electron donor signal in *Rb. sphaeroides* was found to be ≈1.4 times narrower than that of the Bchl cation radical (32). This led to the suggestion that the unpaired electron is shared between two Bchls (33) giving rise to the so-called "special pair" or dimer. This model was confirmed by ENDOR experiments (34, 35). In contrast to *Rb. sphaeroides*, the line width of the electron donor in *R. viridis* shows only a reduction of 1.18 (36). This is interpreted as arising from a less symmetric sharing of the electron distribution in the $Bchl_2$ of

¶These correspond to the L and M branches in the publications of Deisenhofer and co-workers (1–3). In view of the intertwining of the two subunits (e.g., Q_A, which lies on the L branch, binds to the M subunit), we chose to label the cofactors according to their positions relative to the primary and secondary quinones Q_A and Q_B.

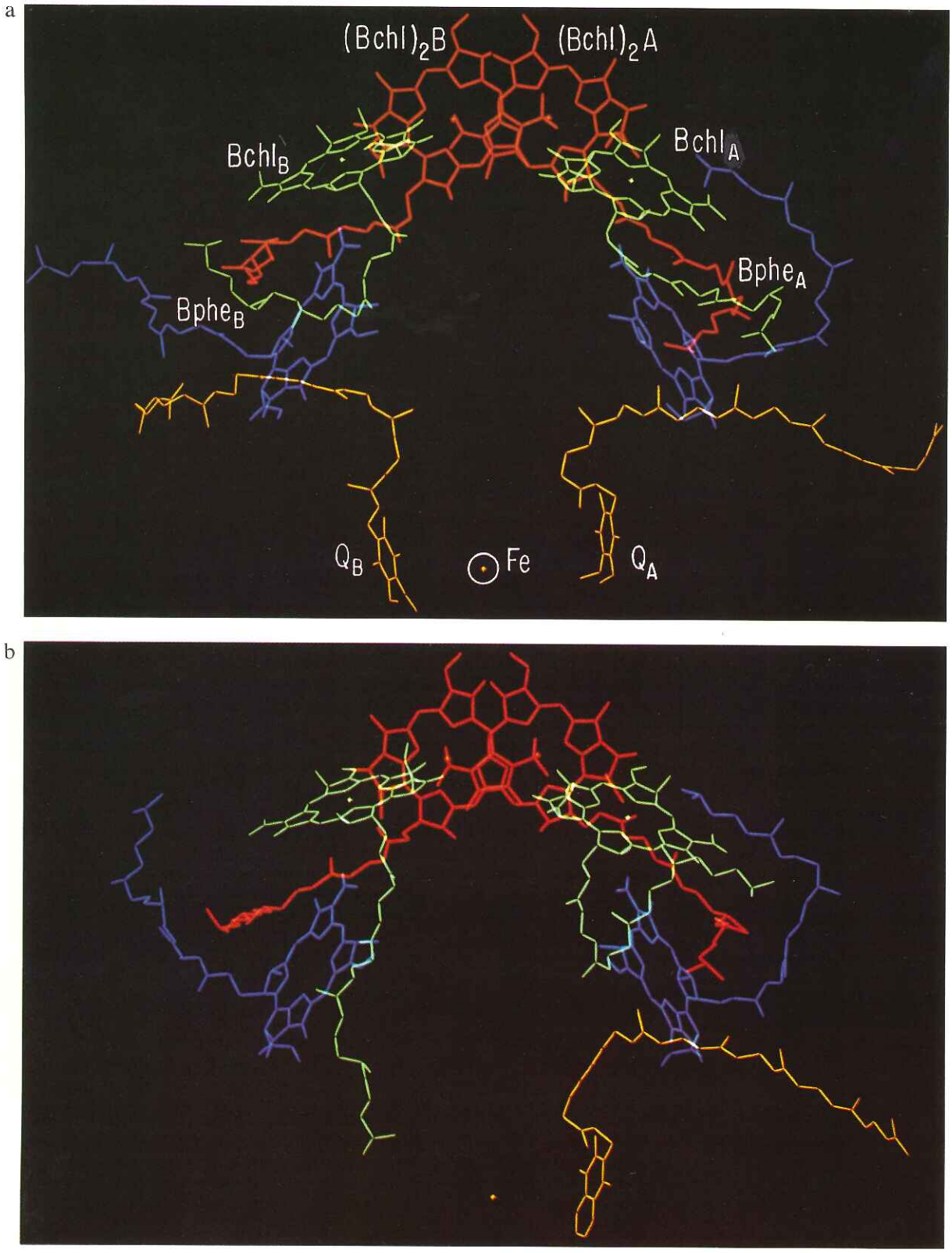

FIG. 1. Cofactor structures of the RC from *Rb. sphaeroides* (*a*) (this work) and from *R. viridis* (*b*) (1, 3). The 2-fold symmetry axis is aligned vertically in the plane of the paper. Electron transfer proceeds preferentially along the A branch. The periplasmic side of the membrane is near the top and the cytoplasmic side is near the bottom of the structure.

R. viridis. Recent ENDOR experiments together with molecular orbital calculations resulted in a model of the dimer consisting of two Bchls related by a C2 symmetry axis with one overlapping ring (37, 38).

The above model is confirmed by the x-ray structure. Comparison of the $Bchl_2$ of the two species shows a strong homology (see Table 1 and Fig. 1). In the RC from both species, the Bchls of the dimer overlap at the ring I positions (1, 14). In *Rb. sphaeroides*, the distance between ring centers is 7.0 Å. The two Bchls are approximately parallel; the angle

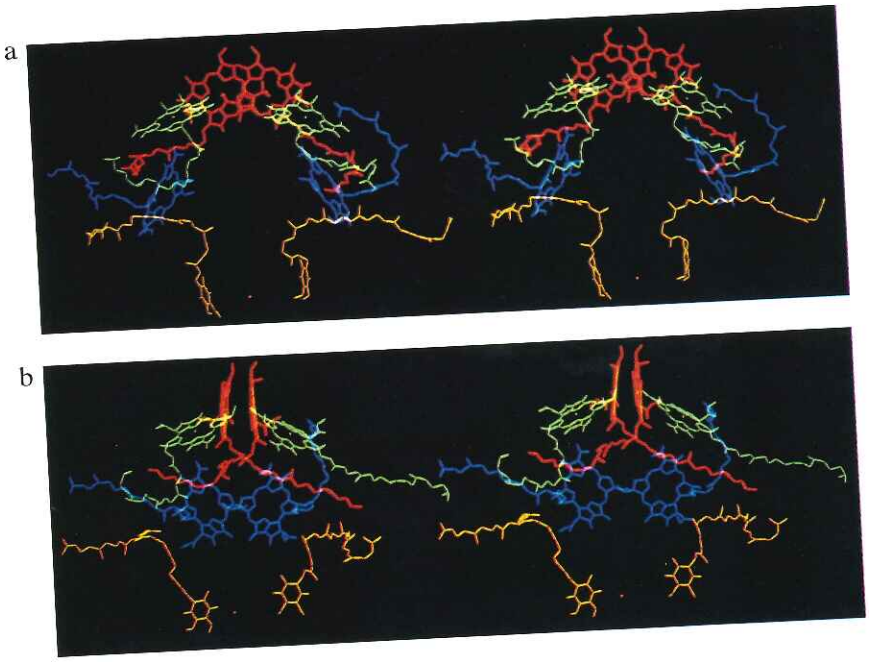

FIG. 2. Stereoplots of the cofactors of the RC from *Rb. sphaeroides*. *b* is related to *a* by a 90° clockwise rotation around the 2-fold symmetry axis with the direction defined from the Fe to the dimer.

between the ring normals is ≈10°. The angle between the lines joining N_1 with N_3 of each Bchl is 140° ± 10° for both bacterial species. This angle $(4/5)\pi$ optimizes the overlap between rings I. The average distance between rings I in *Rb. sphaeroides* is 3.5 Å and in *R. viridis* it is closer to 3 Å.

The acetyl groups of ring I lie approximately in the plane of the Bchls and are located ≈3.5 Å from the central Mg atoms. It was originally postulated that in *R. viridis* the acetyl group was coordinated to the Mg (1). The more recent analysis postulates, in accord with resonance Raman data (39), a 5-coordinated Mg with the acetyl group hydrogen bonded to His L168 and Tyr M195 (3). Similarly, in *Rb. sphaeroides* the respective acetyl groups are within hydrogen bonding distance to His L168 and Tyr M210. It should be noted that the acetyl group forms part of the ring conjugation; consequently, the angle that it makes with respect to the plane of the ring is of great importance. Small conformational changes (e.g., induced by light or temperature variations) may result in relatively large changes in the electronic properties and electron transfer characteristics of the dimer; these changes may even cause a switch from one bonding configuration to another.

The Bchl Monomers. The function of the Bchl monomers has been the subject of considerable debate (for a review, see ref. 29). Although it is now generally accepted that they do not serve as an intermediate acceptor, their presence is believed to play an important role in facilitating electron transfer from $Bchl_2$ to Bphe.

The x-ray structure shows that the Bchl monomers are positioned in each branch between $Bchl_2$ and Bphe (Fig. 1). However, their positioning differs in the two branches. For instance, in *Rb. sphaeroides* the closest approach of ring II of $Bchl_A$ to ring V of $(Bchl_2)_A$ is ≈6.5 Å, whereas the closest approach of ring II of $Bchl_B$ to ring V of $(Bchl_2)_B$ is ≈5.0 Å. Furthermore, the van der Waals overlap (40) between $Bchl_A$ and $(Bchl_2)_B$ is larger by a factor of ≈1.5 than the corresponding overlap between $Bchl_B$ and $(Bchl_2)_A$. Similar asymmetries are present in *R. viridis*. These asymmetries may contribute to the preferential electron transfer along the A branch.

The Bphes. Optical studies have shown that one of the Bphes serves as an intermediate acceptor, while the other is not involved in the electron transfer. The characteristic transfer time from $Bchl_2$ to Bphe in both species at 295 K is ≈4 ps (for review, see ref. 29).

The Bphe is located in each branch between the Bchl monomers and the quinones (see Fig. 1 and Table 1). We identify $Bphe_A$ as the intermediate acceptor since Q_A is considerably closer to $Bphe_A$ than it is to $Bphe_B$. The acetyl groups of both Bphes point toward the $Bchl_2$. The distance between the acetyl group of $Bphe_A$ and ring IV of $(Bchl_2)_A$ is ≈7.0 Å. In the RC from *Rb. sphaeroides*, Tyr M210 is located between $Bchl_2$ and $Bphe_A$. Its possible role in hydrogen bonding has been discussed in a previous section. Here we want to point out that Tyr M210 is in van der Waals contact with rings I of both $(Bchl_2)_B$ and $Bphe_A$; it may, therefore, serve as a conduit for electron transfer from $Bchl_2$ to $Bphe_A$. A similar role may be played in *R. viridis* by the corresponding residue Tyr M208.

The Primary Quinone. The electron transfer proceeds from $Bphe_A$ to the primary quinone in both *Rb. sphaeroides* and *R. viridis* in ≈200 ps at 295 K (28, 29). We identify the primary quinone with Q_A of Fig. 1*a* due to the equivalent location of the menaquinone in *R. viridis* (Fig. 1*b*) and on the basis of photoaffinity labeling experiments (41) and EPR data discussed in a later section.

Q_A receives an electron from $Bphe_A$; the centers of Q_A and $Bphe_A$ are separated by 13 Å (see Table 1). In *Rb. sphaeroides*, the aromatic ring of Trp M252 is located between the rings of these cofactors; its closest approach to the tetrapyrrole ring of $Bphe_A$ is ≈5 Å and to the quinone ring it is 3–5 Å. The structure suggests that Trp M252 plays a likely role in the electron transfer process. The residue Trp M252 is conserved in *R. viridis*, although the distances (and angles) to the cofactors differ somewhat (3).

The Secondary Quinone. The secondary quinone, Q_B, is the final electron acceptor of the RC. When this quinone becomes doubly reduced it interacts with exogenous quinones, thus serving as a two-electron gate (42, 43). In *Rb. sphaeroides* electron transfer occurs from Q_A to Q_B in ≈100 μs at 295 K (28). The separation between the two quinones is 18.5 Å (Table 1). Located between the quinones are the imidazole rings of His M219 and His L190. The separation between neighboring rings is 3–5 Å. This arrangement suggests that these two histidines play a role in the electron transfer from Q_A to Q_B. The two histidines are conserved in the RC of *R. viridis* (His M217 and His L190) (3), although as mentioned before, the putative Q_B site is not occupied by a quinone in the crystals of *R. viridis*.

A striking feature associated with the quinones is the difference of at least 2 orders of magnitude in the direct charge recombination rate of Q_A^- and Q_B^- with $(Bchl)_2^+$ (44).

This is difficult to reconcile with the symmetrical structure shown in Fig. 1*a*, in which the distance between the carbonyl oxygen of Q_A to ring IV of $(Bchl_2)_A$ is approximately the same (≈23 Å) as that of Q_B to $(Bchl_2)_B$. The protein matrix may be responsible for the difference in the recombination rates. Similarly, the asymmetry of the protein matrix may contribute to the preferential electron transport along the A branch.

The Nonheme Iron. The electronic structure of the iron has been investigated by a variety of experimental techniques. These include magnetic susceptibility measurements (45), Mossbauer spectroscopy (46), extended x-ray fine structure absorption (47, 48), and EPR (49, 50). The conclusions about the Fe^{2+} arrived at from these experiments are (*i*) it is in a high spin Fe^{2+} state irrespective of the oxidation state of the quinone acceptors (45, 46); (*ii*) it does not form a direct ligand to the quinones (45–49); (*iii*) it interacts magnetically with the unpaired electron on the quinone (45, 49, 50); (*iv*) its most likely number of ligands is six, with an average bond length of 2.12 ± 0.03 Å (47, 48); (*v*) its environment is a distorted octahedron (45–49); (*vi*) it is closer to Q_B than to Q_A (49). It was originally thought that the Fe^{2+} may play an important role in the electron transfer from Q_A and Q_B (6, 51). However, recent experiments have shown that removal of Fe^{2+} does not significantly affect the rate of electron transfer to Q_B (10). Consequently, other roles for the Fe^{2+} were postulated (10), among them a structural role to be discussed in more detail in a later paper.

The predictions discussed above are supported by the x-ray diffraction data. The Fe^{2+} is located between the two quinones (see Fig. 1*a*). In *Rb. sphaeroides*, it is coordinated to four histidines (L230, L190, M219, and M266) and to the bidentate ligands of Glu M234. All five residues are conserved in *R. viridis* (His L190, L230, M217, and M264; Glu M232) (3). As in *R. viridis* (3), the ligands form a distorted octahedron, and Fe^{2+} in *Rb. sphaeroides* is closer to Q_B than to Q_A by ≈2 Å (see Table 1).

We thank E. Abresch for the preparation of the RCs, M. Y. Okamura for helpful discussions, R. M. Sweet for assistance in the data collection at Brookhaven, and J. Deisenhofer for the FRODO dictionary. This work was supported by grants from the National Institutes of Health (AM36053, GM13191, GM31299, and GM07185), the National Science Foundation (DMB85-18922), a Presidential Young Investigator Award, and the Chicago Community Trust/Searle Scholars Program. The crystallographic station at the Brookhaven National Laboratory was supported by the Department of Energy.

1. Deisenhofer, J., Epp, O., Miki, K., Huber, R. & Michel, H. (1984) *J. Mol. Biol.* **180,** 385–398.
2. Deisenhofer, J., Epp, O., Miki, K., Huber, R. & Michel, H. (1985) *Nature (London)* **318,** 618–624.
3. Michel, H., Epp, O. & Deisenhofer, J. (1986) *EMBO J.* **5,** 2445–2451.
4. Feher, G. & Okamura, M. Y. (1978) in *The Photosynthetic Bacteria*, eds. Clayton, R. K. & Sistrom, W. R. (Plenum, New York), pp. 349–386.
5. Okamura, M. Y., Feher, G. & Nelson, N. (1982) in *Photosynthesis*, ed. Govindjee (Academic, New York), pp. 195–272.
6. Okamura, M. Y., Isaacson, R. A. & Feher, G. (1975) *Proc. Natl. Acad. Sci. USA* **72,** 3491–3495.
7. Gunner, M., Robertson, D. E. & Dutton, P. L. (1986) *J. Phys. Chem.* **90,** 3783–3795.
8. Diston, S. L., Davis, R. C. & Pearlstein, R. M. (1984) *Biochim. Biophys. Acta* **776,** 623–629.
9. Debus, R. J., Feher, G. & Okamura, M. Y. (1985) *Biochemistry* **24,** 2488–2500.
10. Debus, R. J., Feher, G. & Okamura, M. Y. (1986) *Biochemistry* **25,** 2276–2287.
11. Rossman, M. G., ed. (1972) *The Molecular Replacement Method* (Gordon & Breach, New York).
12. Allen, J. P., Feher, G., Yeates, T. O., Rees, D. C., Eisenberg, D. S., Deisenhofer, J., Michel, H. & Huber, R. (1986) *Biophys. J.* **49,** 583a (abstr.).
13. Chang, C. H., Tiede, D., Tang, J., Smith, U., Norris, J. & Schiffer, M. (1986) *FEBS Lett.* **205,** 82–86.
14. Allen, J. P., Feher, G., Yeates, T. O., Rees, D. C., Deisenhofer, J., Michel, H. & Huber, R. (1986) *Proc. Natl. Acad. Sci. USA* **83,** 8589–8593.
15. Allen, J. P. & Feher, G. (1984) *Proc. Natl. Acad. Sci. USA* **81,** 4795–4799.
16. Allen, J. P. & Feher, G. (1984) *Biophys. J.* **45,** 256a (abstr.).
17. Allen, J. P., Feher, G., Yeates, T. O. & Rees, D. C. (1987) in *Progress in Photosynthesis Research*, ed. Biggins, J. (Nijhof/Junk, Brussels, Belgium), Vol. 1, pp. 4.375–4.378.
18. Feher, G. & Allen, J. P. (1985) in *Molecular Biology of the Photosynthetic Apparatus*, eds. Steinback, K. E., Bonitz, S., Arntzen, C. J. & Bogorad, L. (Cold Spring Harbor Laboratory, Cold Spring Harbor, NY), pp. 163–172.
19. Harburn, G., Taylor, C. A. & Welberry, T. R. (1975) *Atlas of Optical Transforms* (Bell, London).
20. Welberry, T. R. & Galbraith, R. (1973) *J. Appl. Crystallogr.* **6,** 87–96.
21. Cork, C., Hamlin, R., Vernon, W. & Xuong, N. H. (1985) *Methods Enzymol.* **114,** 452–472.
22. Reeke, G. N. (1984) *J. Appl. Crystallogr.* **17,** 125–130.
23. Crawford, J. L. (1977) Dissertation (Harvard Univ., Cambridge, MA).
24. Hendrickson, W. A. (1985) *Methods Enzymol.* **115,** 252–270.
25. Jack, A. & Levitt, M. (1978) *Acta Crystallogr.* **A34,** 931–935.
26. Jones, T. A. (1985) *Methods Enzymol.* **115,** 157–171.
27. Luzzati, V. (1953) *Acta Crystallogr.* **6,** 142–157.
28. Parson, W. W. & Ke, B. (1982) in *Photosynthesis*, ed. Govindjee (Academic, New York), pp. 331–385.
29. Kirmaier, C. & Holten, D. (1987) *Photosynth. Res.*, in press.
30. Kabsch, W. (1976) *Acta Crystallogr.* **A32,** 922–923.
31. Smith, D. P. E., Bryant, A., Quate, C. F., Rabe, J. P., Gerber, C. H. & Swalen, J. D. (1987) *Proc. Natl. Acad. Sci. USA* **84,** 969–972.
32. McElroy, J. D., Feher, G. & Mauzerall, D. C. (1969) *Biochim. Biophys. Acta* **172,** 180–183.
33. Norris, J. R., Uphaus, R. A., Crespi, H. L. & Katz, J. S. (1971) *Proc. Natl. Acad. Sci. USA* **68,** 625–628.
34. Feher, G., Hoff, A. J., Isaacson, R. A. & Ackerson, L. C. (1975) *Ann. N.Y. Acad. Sci.* **244,** 239–259.
35. Norris, J. R., Scheer, H. & Katz, J. J. (1975) *Ann. N.Y. Acad. Sci.* **244,** 260–281.
36. Fajer, I., Davis, M. S., Brune, D. C. Spaulding, L. D., Borg, D. C. & Forman, A. (1977) *Brookhaven Symp. Biol.* **28,** 74–103.
37. Lubitz, W., Lendzian, F., Scheer, H., Gottstein, J., Plato, M. & Mobius, K. (1984) *Proc. Natl. Acad. Sci. USA* **81,** 1401–1405.
38. Plato, M., Tränkle, E., Lubitz, W., Lendzian, F. & Möbius, K. (1986) *Chem. Phys.* **107,** 185–196.
39. Zhou, Q., Robert, B. & Lutz, M. (1987) *Biochim. Biophys. Acta* **890,** 368–376.
40. Richards, F. M. (1985) *Methods Enzymol.* **115,** 440–464.
41. Marinetti, T. D., Okamura, M. Y. & Feher, G. (1979) *Biochemistry* **18,** 3126–3133.
42. Vermeglio, A. (1977) *Biochim. Biophys. Acta* **459,** 516–524.
43. Wraight, C. A. (1977) *Biochim. Biophys. Acta* **459,** 525–531.
44. Kleinfeld, D., Okamura, M. Y. & Feher, G. (1984) *Biochim. Biophys. Acta* **766,** 126–140.
45. Bulter, W. F., Johnson, D. C., Shore, H. B., Fredkin, D. R., Okamura, M. Y. & Feher, G. (1980) *Biophys J.* **32,** 967–992.
46. Boso, B., Debrunner, P., Okamura, M. Y. & Feher, G. (1981) *Biochim. Biophys. Acta* **638,** 173–177.
47. Eisenberger, P., Okamura, M. Y. & Feher, G. (1982) *Biophys. J.* **37,** 523–538.
48. Bunker, G., Stern, E. A., Blankenship, R. E. & Parson, W. W. (1982) *Biophys. J.* **37,** 539–551.
49. Butler, W. F., Calvo, R., Fredkin, D. R., Isaacson, R. A., Okamura, M. Y. & Feher, G. (1984) *Biophys. J.* **45,** 947–973.
50. Dismukes, G. C., Frank, H. A., Friesner, R. & Sauer, K. (1984) *Biochim. Biophys. Acta* **764,** 253–271.
51. Blankenship, R. E. & Parson, W. W. (1979) *Biochim. Biophys. Acta* **545,** 429–444.
52. Allen, J. P., Feher, G., Yeates, T. O., Komiya, H. & Rees, D. C. (1987) *Proc. Natl. Acad. Sci. USA* **84,** in press.
53. Yeates, T. O., Komiya, H., Rees, D. C., Allen, J. P. & Feher, G. (1987) *Proc. Natl. Acad. Sci. USA* **84,** in press.